**The EMBO Journal (2009) 28,** 2825–2834 | © 2009 European Molecular Biology Organization | All Rights Reserved 0261-4189/09
www.embojournal.org

THE EMBO JOURNAL

# Coupling of activation and inactivation gate in a $K^+$-channel: potassium and ligand sensitivity

**Christian Ader[1,4], Robert Schneider[2,4], Sönke Hornig[3], Phanindra Velisetty[3], Vitya Vardanyan[3], Karin Giller[2], Iris Ohmert[3], Stefan Becker[2,*], Olaf Pongs[3,*] and Marc Baldus[1,*]**

[1]Bijvoet Center for Biomolecular Research, Utrecht University, Utrecht, The Netherlands, [2]Department of NMR-Based Structural Biology, Max-Planck-Institute for Biophysical Chemistry, Göttingen, Germany and [3]University-Hospital Hamburg-Eppendorf, Center for Molecular Neurobiology, Institute for Neural Signaltransduction, Hamburg, Germany

**Potassium ($K^+$)-channel gating is choreographed by a complex interplay between external stimuli, $K^+$ concentration and lipidic environment. We combined solid-state NMR and electrophysiological experiments on a chimeric KcsA–Kv1.3 channel to delineate $K^+$, pH and blocker effects on channel structure and function in a membrane setting. Our data show that pH-induced activation is correlated with protonation of glutamate residues at or near the activation gate. Moreover, $K^+$ and channel blockers distinctly affect the open probability of both the inactivation gate comprising the selectivity filter of the channel and the activation gate. The results indicate that the two gates are coupled and that effects of the permeant $K^+$ ion on the inactivation gate modulate activation-gate opening. Our data suggest a mechanism for controlling coordinated and sequential opening and closing of activation and inactivation gates in the $K^+$-channel pore.**

*The EMBO Journal* (2009) **28,** 2825–2834. doi:10.1038/emboj.2009.218; Published online 6 August 2009
*Subject Categories*: membranes & transport; structural biology
*Keywords*: ion-channel gating; $K^+$-channel; membrane protein; pH sensor; solid-state NMR

## Introduction

Potassium ($K^+$)-channel activation has an important function in neural signal transduction, as it regulates selective conduction of $K^+$ across biological membranes (Hille, 2001). In response to changes in chemical or electrical potential, the pore domain of $K^+$-channels opens and closes, thereby controlling $K^+$ access to the pore (Yellen, 1998; Armstrong, 2003). $K^+$ channels have a common pore design, which includes the presence of an activation gate at the intracellular entrance of the pore and of a separate inactivation gate situated towards the extracellular entrance at the selectivity filter. Gating of the $K^+$ channel involves structural rearrangements at the two gates. The activation gate is associated with the inner-helix bundle that moves during activation around a gating hinge (Liu *et al*, 1997, 2001; Doyle *et al*, 1998; Holmgren *et al*, 1998; Perozo *et al*, 1998, 1999; Jiang *et al*, 2002a, b; Kelly and Gross, 2003; Ader *et al*, 2008), whereas closing of the inactivation gate concurs with rearrangements at the selectivity filter to enter an inactivated state of the $K^+$ channel (Liu *et al*, 1996; Zheng and Sigworth, 1997; Kiss and Korn, 1998; Ogielska and Aldrich, 1999; Bernèche and Roux, 2005; Gao *et al*, 2005; Blunck *et al*, 2006; Kurata and Fedida, 2006; Cordero-Morales *et al*, 2006a, b, 2007; Chakrapani *et al*, 2007a, b; Ader *et al*, 2008). In the family of voltage-gated $K^+$ (Kv) channels, opening and closing of activation and inactivation gate were shown to be coupled (Baukrowitz and Yellen, 1995, 1996; Panyi and Deutsch, 2006, 2007). It is likely that coupling between the two gates ensures maximum channel open probability and also sequentially coordinates activation and inactivation gating of the $K^+$ channel.

The bacterial $K^+$-channel KcsA (Schrempf *et al*, 1995; Perozo *et al*, 1998; Zhou *et al*, 2001) provides a powerful and robust model system for a detailed investigation of channel gating. Studies of KcsA mutants have identified amino-acid residues involved in KcsA-channel gating (Cordero-Morales *et al*, 2007; Thompson *et al*, 2008). In the resting state, the activation gate of the channel is closed and the inactivation gate is opened, that is the selectivity filter has a conductive structure. Acidic pH elicits activation-gate opening and thus an activated state of the KcsA channel (Perozo *et al*, 1999; Liu *et al*, 2001; Blunck *et al*, 2006; Cordero-Morales *et al*, 2006b; Baker *et al*, 2007; Ader *et al*, 2008). The state is short-lived because the inactivation gate rapidly closes the filter of the activated $K^+$ channel. According to solid-state (ss) NMR spectroscopy (Ader *et al*, 2008), the inactivated-filter conformation shares essential features with the collapsed or non-conductive-filter structure seen in KcsA-crystal structures obtained in low [$K^+$] (Zhou *et al*, 2001; Lenaeus *et al*, 2005; Lockless *et al*, 2007).

The influence of external [$K^+$] on selectivity-filter stability and $K^+$-channel gating, for example C-type inactivation of *Shaker* channels, has been extensively studied on a functional level (Zagotta and Aldrich, 1990; Demo and Yellen, 1991; Kiss and Korn, 1998; Claydon *et al*, 2007; Chakrapani *et al*, 2007b). However, how sequential gating activity of the two gates in the $K^+$-channel pore domain is choreographed and affected by the permeant ions is not well understood. A comprehensive understanding of channel gating, hence, should involve structural studies that delineate the cumulative

*Corresponding authors. M Baldus, Bijvoet Center for Biomolecular Research, Utrecht University, Padualaan 8, 3584 CH Utrecht, The Netherlands. Tel.: +31 030 253 3801; Fax: +31 030 253 7623; E-mail: m.baldus@uu.nl or S Becker, Max-Planck-Institute for Biophysical Chemistry, Am Fassberg 11, 37077 Göttingen, Germany, Tel.: +49 551 201 2222; Fax: +49 551 201 2202; E-mail: sabe@nmr.mpibpc.mpg.de or O Pongs; Institute for Neural Signaltransduction, Falkenried 94, 20251 Hamburg, Germany. Tel.: +49(0)40 7410 5 5081, Fax: +49(0)40 7410 5 6643; E-mail: morin@zmnh.uni-hamburg.de
[4]These authors contributed equally to this work

**Received: 27 March 2009; accepted: 8 July 2009; published online: 6 August 2009**

effect of pH and $K^+$ concentration in a functional lipidic environment. We have earlier shown that under such conditions, high-resolution ssNMR spectroscopy is a sensitive method for analysing ligand binding (Lange *et al*, 2006; Ader *et al*, 2008), conformational changes related to pH-induced activation and inactivation gating (Ader *et al*, 2008, 2009b) and site-resolved dynamics of a membrane embedded $K^+$ channel (Ader *et al*, 2009a). Here, we used ssNMR chemical-shift mapping in direct reference to electrophysiological recordings on KcsA–Kv1.3 preparations to dissect the pH, $K^+$ and ligand sensitivity of channel gating. KcsA–Kv1.3 contains a high-affinity-binding site for the scorpion toxin kaliotoxin (KTX), which was generated by replacing 11 amino-acid residues in the extracellular loop of the KcsA pore domain by those of Kv1.3 (Legros *et al*, 2000, 2002).

We found that pH-induced gating of KcsA–Kv1.3 is modulated by the concentration of external as well as internal $K^+$. Correspondingly, distinct $K^+$-binding events affect inactivation and activation gating of the $K^+$ channel. Using ssNMR, we studied these gating states in lipid bilayers by tracking $K^+$- and pH-dependent changes in protein conformation and side-chain protonation. Moreover, we probed coordinated actions of opening and closing of the two gates by trapping the $K^+$ channel in distinct states with external pore blockers (Lange *et al*, 2006; Ader *et al*, 2008). We observed that pH, $K^+$ and the scorpion toxin KTX markedly influence the open probability of the activation gate. Although the effect of pH relates to protonation of glutamate residues located in the intracellular 'pH sensor' of the channel, the effects of $K^+$ and KTX are mediated through distinct-binding sites within or near the selectivity filter. We show that the inactivation gate can influence activation gating and that coupling between the two gates allows for a choreographed response to $K^+$. The findings suggest that the permeant $K^+$ ion itself regulates onset of $K^+$-channel activation as well as inactivation. We propose that a self-regulatory mechanism controls sequential gating activity in a $K^+$ channel.

## Results

### *Gating is modulated by internal and external $K^+$*

We can depict KcsA–Kv1.3-channel gating with a simplified gating cycle describing equilibria between four composite gating states, namely closed-state C, opened-state O and inactivated states I and I* (Figure 1A) (Yellen, 1998; Panyi and Deutsch, 2006; Ben-Abu *et al*, 2009). On the basis of earlier work on KcsA (LeMasurier *et al*, 2001; Zakharian and Reusch, 2004), we hypothesized that the equilibria between the four $K^+$-channel states have different sensitivities to internal ($[K^+]_{in}$) and external ($[K^+]_{out}$) $K^+$ concentrations. Therefore, we investigated effects of changes in $[K^+]_{in}$ and $[K^+]_{out}$ on pH-induced KcsA–Kv1.3-channel gating.

First, we studied the influence of $[K^+]_{out}$ on KcsA–Kv1.3-channel inactivation by establishing inside-out patches from KcsA–Kv1.3 proteoliposomes prepared in 150 mM NaCl. The pipette solution (corresponding to $[K^+]_{out}$) was varied between 0 and 150 mM KCl. The bath solution was set to 150 mM KCl ($[K^+]_{in}$). As earlier described (Cuello *et al*, 1998; Chakrapani *et al*, 2007a, b), a change in pH from 7.5 to 4.0 activates the KcsA–Kv1.3 channel, and in the continued

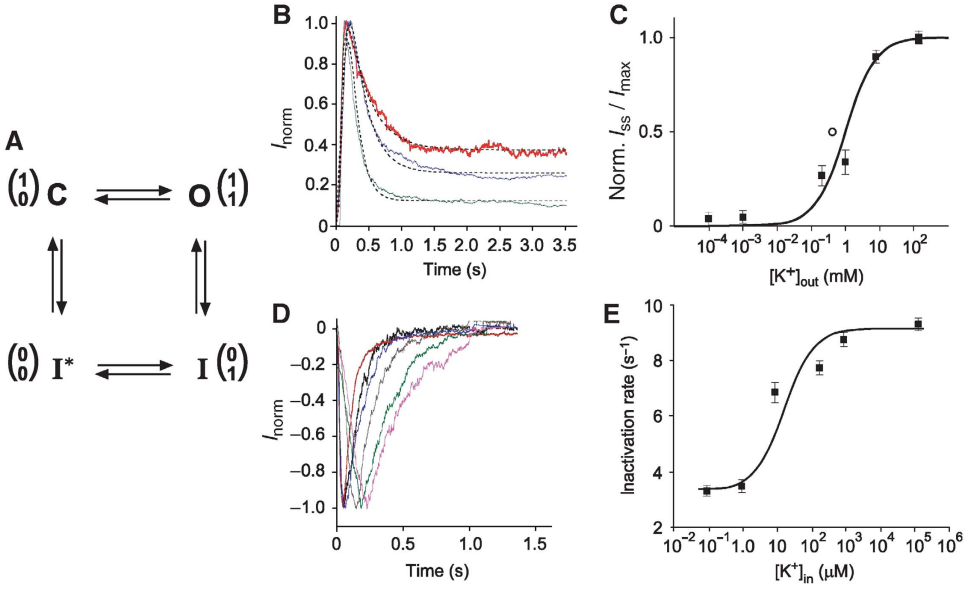


**Figure 1** $K^+$ sensitivity of KcsA–Kv1.3-channel gating. (**A**) A four-state minimal gating model with an upper (inactivation) and a lower (activation) gate in the conduction pathway of the KcsA–Kv1.3 channel. Gate positions (0 for closed and 1 for opened) are diagrammed in one-column matrices with upper gate in upper and lower gate in lower row. C—closed channel in resting state; O—opened channel; I and I*—inactivated states. (**B**) Normalized KcsA–Kv1.3 outward currents ($I_{norm}$) recorded at +100 mV with different external $K^+$ ($[K^+]_{out}$) concentrations (150 mM, red; 1 mM, blue; 1 μM, green). Inside (bath) solution contained always 150 mM KCl. Dashed curves are fits to the data according to Roeper *et al* (1997). (**C**) Normalized steady-state current amplitudes $(I_{ss})_{norm}$ plotted against $[K^+]_{out}$. Solid line represents fitted curve to the dose-response data (■) with $K_D$ for external $K^+$ binding of 0.9 mM. Error bars are s.e.m. ($n = 5$–14). (○)—$K_D$ for extracellular $K^+$-binding site on KcsA (Lockless *et al*, 2007). (**D**) Normalized KcsA–Kv1.3 inward currents ($I_{norm}$) recorded at −100 mV with different internal $K^+$ ($[K^+]_{in}$) solutions (0 mM, magenta; 1 μM, green; 10 μM, brown; 0.2 mM, black; 1 mM, blue; 150 mM, red). Outside (pipette) solution contained 150 mM KCl. (**E**) $[K^+]_{in}$ sensitivity of inactivation rate. Error bars are s.e.m. ($n = 5$–12). $K_D$ value of 6.5 μM was obtained by fitting a smooth curve to the dose-response data (■) as described by Baukrowitz and Yellen (1996) (for further details see Supplementary data).

 

presence of protons, the activated channel slowly inactivates, reflecting a conformational transition from a conductive to a non-conductive state, and finally reaches a steady-state current ($I_{ss}$) level (Figure 1B) (Ader *et al*, 2008). Currents were well described by fitting to the data a Hodgkin—Huxley-related formalism ($I = I_0 m(t)^4 h(t)$) with one activation ($\tau_{act}$) and one inactivation time constant ($\tau_{inact}$) (Roeper *et al*, 1997). The time constants $\tau_{act}$ and $\tau_{inact}$ varied with $[K^+]_{out}$ (Supplementary Table 1). Moreover, KcsA–Kv1.3 steady-state current levels ($I_{ss}/I_{max}$), remaining at the end of the test pulse, were very sensitive to $[K^+]_{out}$ (Figure 1B). A plot of $I_{ss}/I_{max}$ versus $[K^+]_{out}$ revealed that $I_{ss}/I_{max}$ titrates with $[K^+]_{out}$ (Figure 1C), showing a $K_D$ of 0.9 mM with a maximal $I_{ss}/I_{max}$ value of 0.44 at 150 mM $[K^+]_{out}$ and a minimum $I_{ss}/I_{max}$ value of 0.02 at 0 $[K^+]_{out}$ (Supplementary Table 1). We note that this $K_D$ value of $K^+$-sensitive KcsA–Kv1.3 inactivation is similar to the $K_D$ of 0.43 mM determined in calorimetric studies for an external $K^+$-binding site of the closed KcsA channel (Lockless *et al*, 2007). Importantly, $K^+$ occupancy of this site affects selectivity-filter conformation. Therefore, the conclusion is that $K^+$ binding to this site is essential for a stable-conductive structure of the selectivity filter, which otherwise is prone to collapse (Zhou *et al*, 2001; Bernèche and Roux, 2005; Lockless *et al*, 2007).

Next, we investigated the influence of $[K^+]_{in}$ on KcsA–Kv1.3 gating properties. Inside-out patches were established with 150 mM $K^+$ in the pipette solution and were perfused with bath solution containing different $[K^+]_{in}$ (0–150 mM $K^+$). On a pH jump from 7.5 to 4.0, hyperpolarizing test pulses induced rapid activation of $K^+$ inward current (Figure 1D). In agreement with earlier reported outward-rectification properties of KcsA-mediated currents, inactivation of KcsA–Kv1.3 inward current was essentially complete (Heginbotham *et al*, 1999; Chakrapani *et al*, 2007b). The most important observation, which we made in the data was that $[K^+]_{in}$ significantly accelerated KcsA–Kv1.3 inactivation with a minimal time constant $\tau_{inact}$ at $\geqslant$0.2 mM $[K^+]_{in}$ (Figure 1D and E; Supplementary Table 2). A plot of $1/\tau_{inact}$ versus $[K^+]_{in}$ showed that $\tau_{inact}$ titrates with $[K^+]_{in}$ (Figure 1E), revealing an internal $K^+$-binding site with $K_D = 6.5\,\mu M$. In contrast, the time course of KcsA–Kv1.3 recovery from inactivation was $K^+$ insensitive. Time constants for recovery from inactivation ($\tau_{rec}$) were in symmetrical (150 mM), low (1 μM) internal or low (1 μM) external $[K^+]$ essentially identical ($\tau_{rec} = 3.24 \pm 0.14$ s, $n = 18$, s.e.m.) (Supplementary Table 3).

The data shows that KcsA–Kv1.3-channel inactivation is over 100-fold more sensitive to $[K^+]_{in}$ than to $[K^+]_{out}$. It suggested that occupation of an internal and external $K^+$-binding site modulates KcsA–Kv1.3-channel gating. This implies that equilibria between activated and inactivated channel states, which are influenced by changes in $[K^+]_{in}$ and $[K^+]_{out}$, are correlated with $K^+$-sensitive conformational rearrangements in the KcsA–Kv1.3 channel. To investigate this $K^+$ sensitivity of KcsA–Kv1.3 conformational states on a structural level, we used ssNMR spectroscopy to obtain information on KcsA–Kv1.3 in the presence of different $K^+$ concentrations.

### *Steady-state KcsA–Kv1.3 conformation at pH 4.0 is $K^+$ sensitive*

We recorded ssNMR spectra of KcsA–Kv1.3 proteoliposomes prepared at different $K^+$ concentrations (0–150 mM) and pH values. The overall ionic strength of the buffers was kept constant in all samples by replacing $K^+$ with sodium. In low $K^+$ concentrations (<1 mM), we had observed sizable chemical-shift changes between pH 7.5 and 4.0. Isotropic chemical shifts for pore-domain residues, for example Glu71, Thr74, Thr75, Val76, Gly77, Tyr78, Gly79, Asp80, Gly99, Ile100 and Thr101 indicated a pore structure in which the activation gate had opened by a bend in the TM2 helix and the selectivity filter had adopted a collapsed conformation (Figure 2A blue bars; Figure 2B blue spectrum) (Ader *et al*, 2008). Strikingly, spectra measured at pH 4.0 and $K^+$ concentrations $\geqslant$10 mM $K^+$ displayed resonances essentially identical to those recorded at pH 7.5, both in phosphate/citrate and MOPS buffers (Figure 2A red bars; Figure 2C red spectrum; Supplementary Figure 1). Similar observations were made for C-terminally truncated KcsA–Kv1.3 comprising only residues 1–125 (Supplementary Figure 1).

Activation-gate opening of $K^+$ channels is associated with an outward movement of the inner (TM2) helices around a gating hinge (Perozo *et al*, 1999; Jiang *et al*, 2002b; Kelly and Gross, 2003; Ader *et al*, 2008). This relatively large conformational change (Liu *et al*, 2001; Kelly and Gross, 2003) consequently increases the water-accessible surface of the channel, particularly of the inner half of the pore domain, and provided an independent means to study activation-gate opening of the KcsA–Kv1.3 channel at acidic pH. We evaluated the water-accessible channel surface by measuring magnetization transferred from selectively excited water protons to channel-protein spins (Ader *et al*, 2009b). The results obtained from this type of NMR experiment are bar graphed in Supplementary Figure 2. In line with our secondary chemical-shift analysis, the data are compatible with a closed-conductive $K^+$-channel conformation prevailing at 50 mM $[K^+]$ across the entire pH range of 4.0–7.5. In contrast, water-edited ssNMR data in low $K^+$ concentrations (<1 mM, Supplementary Figure 2) suggest a marked conformational change of the channel after a shift to acidic pH, and lend independent support to our observation that in the absence of $K^+$, acidic pH induces a conformational change characterized by a stably opened activation gate.

These ssNMR results had two important implications. First, acidic pH, which opens the KcsA–Kv1.3 channel, renders the selectivity-filter vulnerable to inactivation. Second, the probability of activation-gate opening at acidic pH is $K^+$ sensitive. The data show that the prevailing KcsA–Kv1.3 conformation observed at pH 4.0 shifts from the open-collapsed (I) state to the closed-conductive (C) state of the channel (Figure 2D) in the presence of high millimolar $K^+$ concentrations. This complements our electrophysiological studies on the $K^+$ dependency of KcsA–Kv1.3-channel inactivation and shows that both activation and inactivation gate of KcsA–Kv1.3 respond to changes in $K^+$ concentration at a structural level.

### *Conformational changes are associated with glutamate protonation*

Mutational studies suggested that activation-gate opening at acidic pH is associated with protonation of glutamate side chains, notably Glu118 and Glu120 at the lower end of the inner TM2 helix of KcsA (Thompson *et al*, 2008). The isotropic chemical shift of glutamate δ carbon atoms is correlated with the side-chain protonation state (Keim *et al*,

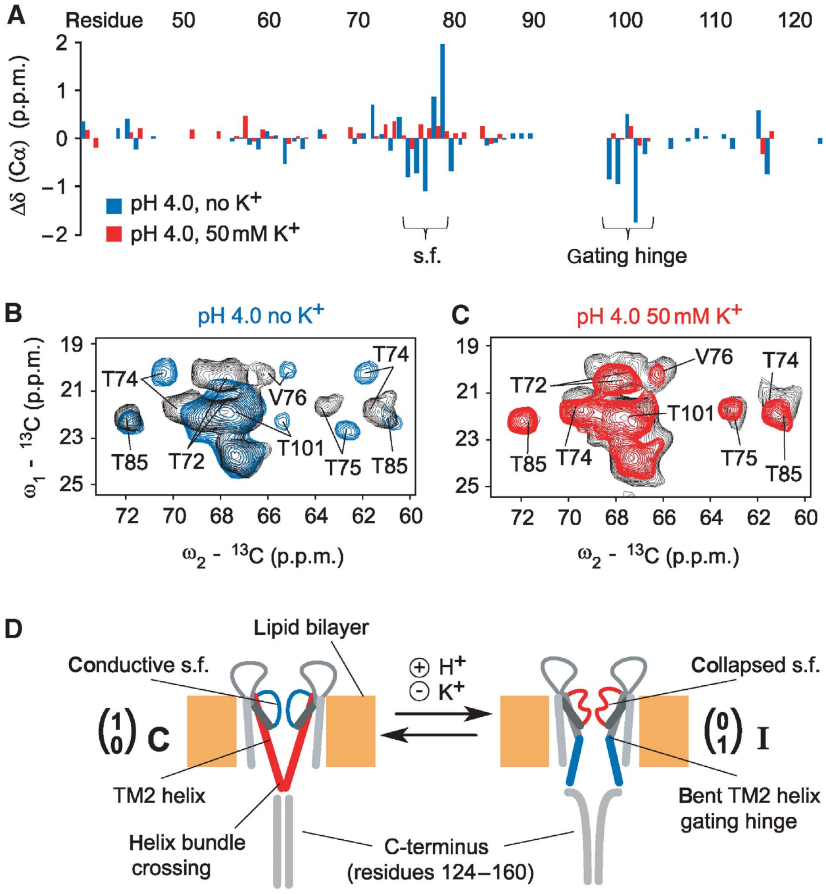


**Figure 2** (**A**) Cα chemical-shift changes observed for the pore domain of KcsA–Kv1.3 (residues 38–122) at pH 4.0 in the absence (blue bars) and the presence of 50 mM [$K^+$] (red bars) compared with values at pH 7.5 plotted against the residue number. Residues comprising the selectivity filter (s.f.) and the gating hinge in TM2 are indicated. **(B)** Regions from ($^{13}C$, $^{13}C$) correlation spectra obtained for KcsA–Kv1.3 at pH 7.5 (black) and pH 4.0 (blue) in the absence of $K^+$. Sizable chemical-shift changes for residues in selectivity filer (T74, T75, V76) and gating hinge (T101) are visible. (**C**) Regions from ($^{13}C$, $^{13}C$) correlation spectra obtained for KcsA–Kv1.3 at pH 7.5 (black) and pH 4.0 (red) in the presence of 50 mM [$K^+$]. No sizable chemical-shift changes are observed. (**D**) Cartoon representation for two subunits of KcsA–Kv1.3 in a lipid bilayer setting. Core elements of gating states are marked. The selectivity filter acts as inactivation gate and resides in conductive/open and collapsed/closed states. The activation gate is located in the TM2 helix of each subunit and gate opening is associated with a bent helix. The C-terminus can be removed by chymotrypsin digestion after reconstitution in lipid bilayers. $H^+$ induces gating transitions, whereas $K^+$ stabilizes the closed-conductive resting state of KcsA–Kv1.3.

1973). Thus, we investigated the influence of pH and $K^+$ on NMR-resonance frequencies of KcsA–Kv1.3 glutamate residues to monitor activation-gate opening. KcsA–Kv1.3 subunits contain each nine glutamates, four in the pore domain (Glu51, 71, 118 and 120) and five in the cytoplasmic C-terminus (Supplementary Figure 3A). Figure 3A–C depicts sections of ($^{13}C$, $^{13}C$) correlation spectra showing glutamate Cγ-Cδ crosspeaks providing information about glutamate protonation states present at different pH and $K^+$ conditions. The chemical shifts of Cδ resonances suggested that all glutamates but Glu71 were at pH 7.5 in a deprotonated and at pH 4.0, in the absence of $K^+$, in a more protonated state (Figure 3A and B). Note that magnitudes of chemical-shift changes are significantly larger than those observed in earlier pH-dependent NMR studies of KcsA in solution (Baker *et al*, 2007; Takeuchi *et al*, 2007). The histidine residue in the outer transmembrane helix (His25), which was shown to be involved in activation gating (Takeuchi *et al*, 2007; Thompson *et al*, 2008), could not be resolved in ssNMR spectra of KcsA–Kv1.3 (Schneider *et al*, 2008). The Glu71-Cδ resonance at pH 7.5 is consistent with a protonated glutamate side chain in agreement with a water-mediated hydrogen bond between Glu71 and Asp80 stabilizing the selectivity filter (Zhou *et al*, 2001; Cordero-Morales *et al*, 2007). We observed at pH 4.0 in the presence of >10 mM [$K^+$] two new glutamate Cγ-Cδ crosspeaks in addition to those earlier assigned to Glu51 and Glu71 (Schneider *et al*, 2008) (Figure 3C). Comparison of ssNMR spectra of full length and C-terminally truncated KcsA–Kv1.3 (Supplementary Figure 3B and C) showed that removal of the C-terminus selectively eliminated one of these two glutamate Cγ-Cδ crosspeaks. This peak was, therefore, assigned to the five C-terminal glutamates and the remaining one to Glu118 and Glu120 (Figure 3C; Supplementary Figure 3B and C).

Following throughout our titration experiments, we monitored relative intensities of Cγ-Cδ crosspeaks corresponding either to more protonated or deprotonated glutamate side chains (Figure 3A–D), and we made the following observations. First, Glu51, having an exposed localization in the extracellular turret region, and the C-terminal glutamates were protonated at pH 4.0 as expected for water-exposed glutamate side chains. We conclude that side-chain protona-

 

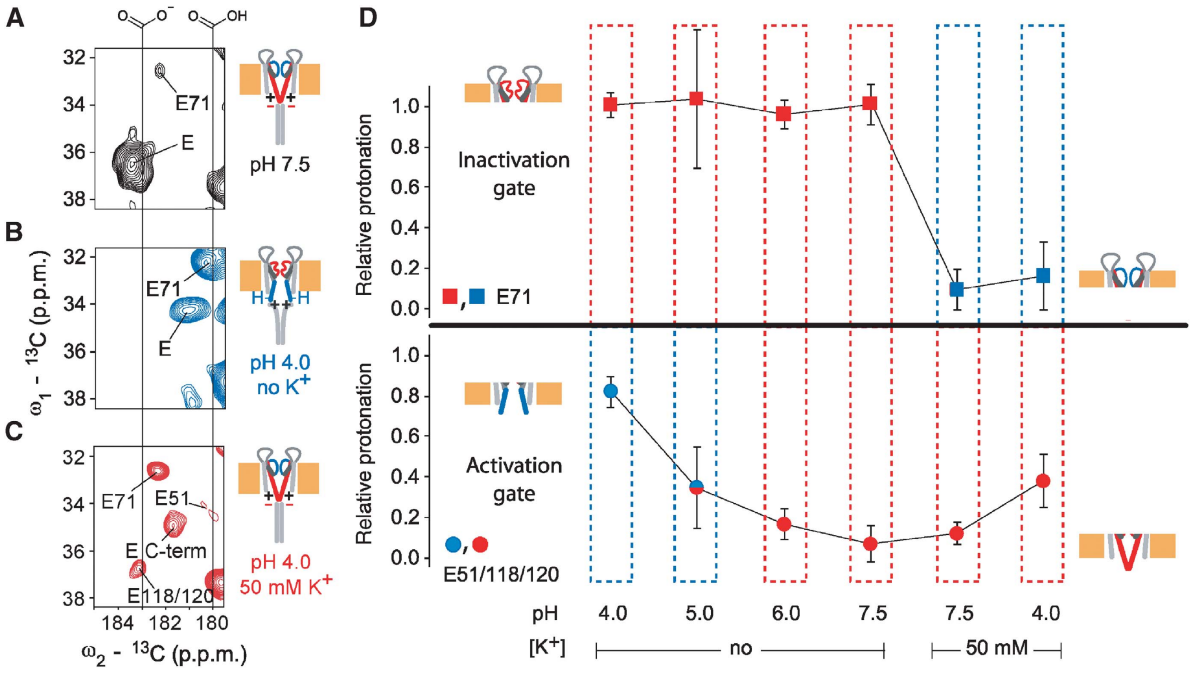


**Figure 3** Protonation of glutamate side-chain carboxyls depends on pH and $[K^+]$. (**A–C**) Regions from ($^{13}C$,$^{13}C$) correlation spectra showing glutamate Cγ-Cδ crosspeaks for different pH and $[K^+]$ conditions. Individual cartoons indicate channel states as defined in Figure 1D. Negative charges and protons illustrate the protonation states of Glu118 and Glu120 at the helix bundle crossing. Positive charges are added to indicate electrostatics at the helix bundle crossing. (**D**) Relative protonation of E71 (squares) and E51/118/120 (circles) computed for different pH and $[K^+]$ conditions for truncated KcsA–Kv1.3 (residues 1–125). For each condition, integrals of crosspeaks corresponding to the respective protonated and deprotonated glutamate Cγ-Cδ crosspeaks were normalized to their sum. Relative protonation is, therefore, represented by the fractions of protonated Cγ-Cδ signal. The colours blue and red indicate open and closed conformations of the channel gates, respectively, as seen by chemical-shift analysis and water-edited spectroscopy. At pH 5.0, in the absence of $K^+$, the state of the activation gate is ambiguous, because many indicative peaks could not be detected in the spectra under these conditions. Drawings indicate gating states as defined in Figure 1D. Protonation of E118/120 correlates with activation-gate opening, whereas inactivation-gate closure involves an increased protonation of E71.

tion of these glutamates is $K^+$ insensitive. In contrast, Cδ resonances of pore-domain glutamates 71, 118 and 120 were markedly $K^+$ sensitive at acidic pH. Their side-chain chemical shifts remained at values seen for neutral pH even at pH 4.0 in the presence of 50 mM $[K^+]$, whereas they shifted to values corresponding to full protonation in the absence of $K^+$. The data show that protonation is $K^+$ sensitive for pore-domain glutamates having important roles in activation (Glu118 and Glu120) (Thompson *et al*, 2008) and inactivation (Glu71) gating of KcsA (Cordero-Morales *et al*, 2006b, 2007) and show that protonation of pore-domain glutamates is associated both with an opened activation gate and collapse of the selectivity filter.

### *Activation and inactivation gate are coupled*

Next, we followed conformational changes in the opened-collapsed channel on back titration from pH 4.0 to 7.5 in the absence of $K^+$ (Figure 3D). We obtained ssNMR spectra revealing a channel conformation with a collapsed selectivity filter and a closed activation gate. Residues of gating hinge, lower pore helix and turret region had returned to their conformational states originally observed at neutral pH (Supplementary Figure 4). Cα and Cβ chemical shifts indicate a backbone conformation associated with the collapsed filter, whereas side-chain resonances of Thr72–Thr75 within the lower selectivity filter and pore helix acquired values close to those seen at pH 7.5. Thus, we identified a closed-collapsed conformation in addition to a closed conductive and an opened-collapsed conformation of the channel. This observation is in agreement with the four-state gating circle depicted in Figure 1A, predicting that the inactivated state comes in two flavours, having either an opened (I) or a closed lower gate (I*). Side-chain resonances of the lower selectivity filter and pore helix (Thr72–Thr75) are only seen to shift together with resonances originating from the gating hinge. This suggests that these side chains are part of an interaction network coupling inactivation and activation gate. Importantly, we could fully restore the closed-conductive (C) state of the $K^+$ channel at pH 7.5 by adding 50 mM $[K^+]$ to the buffer (Figure 3D; Supplementary Figure 4).

### *Ligand-binding unmasks gate coupling*

The inactivation gate comprising the selectivity filter is a prime candidate for locating the $K^+$-binding sites, which influence channel gating as evident from our functional and structural data. To test whether gate coupling conveys $K^+$ sensitivity from the inactivation gate to the activation gate, we used two ligands, which affect KcsA–Kv1.3 selectivity-filter conformation in different ways. The first one, a tetraphenylporphyrin derivative (porphyrin), which binds to KcsA–Kv1.3 with nanomolar affinity, induces a collapsed, non-conductive conformation of the selectivity filter (Ader *et al*, 2008). Binding of the second one, KTX, only affects upper selectivity-filter residues (Lange *et al*, 2006) and stabilizes a conductive filter conformation (Zachariae *et al*, 2008). This particular situation made it possible to study the effect of

acidic pH on the lower activation gate in the context of an opened or a closed upper inactivation gate.

First, we recorded ssNMR spectra from the porphyrin–KcsA–Kv1.3 complex at pH 4.0 in the absence of $K^+$. The spectra were similar to those obtained for the unliganded channel, that is they indicated an open-collapsed structure, exhibiting an opened lower activation gate and a closed upper inactivation gate (Figure 4A). Therefore, the porphyrin-bound channel resides in a closed-collapsed conformation at pH 7.5 and an open-collapsed conformation at pH 4.0 resembling the two inactivated states postulated in the cyclic gating model in Figure 1A. Again, we find that Cα and Cβ chemical shifts of residues Thr72–Thr75 in the lower selectivity filter and pore helix correlate with the open and closed state of the inactivation gate, whereas side-chain chemical shifts on the other hand correlate with the open and closed state of the activation gate (Figure 4A). This suggests that side-chain interactions between residues Thr72–Thr75 in and near the inactivation gate and likely Ile100 in the gating hinge, which shows sizable chemical-shift changes on gate opening (Ader *et al*, 2008), couple the two gates.

Second, we obtained ssNMR spectra from KTX-bound KcsA–Kv1.3. The data revealed that the lower activation gate remained closed at pH 4.0 even in the absence of external $K^+$ (Figure 4B and C). Cδ shifts of Glu118 and Glu120 remained at values corresponding to deprotonated carboxyl groups, whereas C-terminal glutamates exhibited resonances pointing to protonated carboxyl groups. The lower selectivity filter preserved its conductive conformation, and chemical shifts observed for residues 71, 78, 79 and 80 confirmed that KTX remained bound to KcsA–Kv1.3 at pH 4.0 (Figure 4C). The data indicate that KTX binding and high $K^+$ concentrations have analogous effects on KcsA–Kv1.3 gating states, preserving the channel in a closed-conductive conformation in the steady state even at pH 4.0. Table I provides a summary of gating and protonation states observed for free and ligand-bound KcsA–Kv1.3 under different [$K^+$] and pH conditions.

## Discussion

KcsA-channel gating is sensitive to different environmental changes, for example in pH, voltage and $K^+$. Our results provide major insights on how the passage of $K^+$ along the conduction pathway modulates the conformational transitions between opened and closed activation and inactivation gates in a functional membrane setting. We combined ssNMR-titration experiments and electrophysiology to probe the $K^+$ and ligand sensitivity of these gating states and directly followed protonation events accounting for pH-induced channel gating in the KcsA–Kv1.3 $K^+$ channel. With these studies, we obtained spectroscopic information for three of the four major gating states: closed conductive (C), open collapsed (I) and closed collapsed (I*).

The open probabilities of both activation gate and inactivation gate were found to be distinctly $K^+$ sensitive. ssNMR results showed that the closed-conductive conformation of the KcsA–Kv1.3 channel is quantitatively converted to an

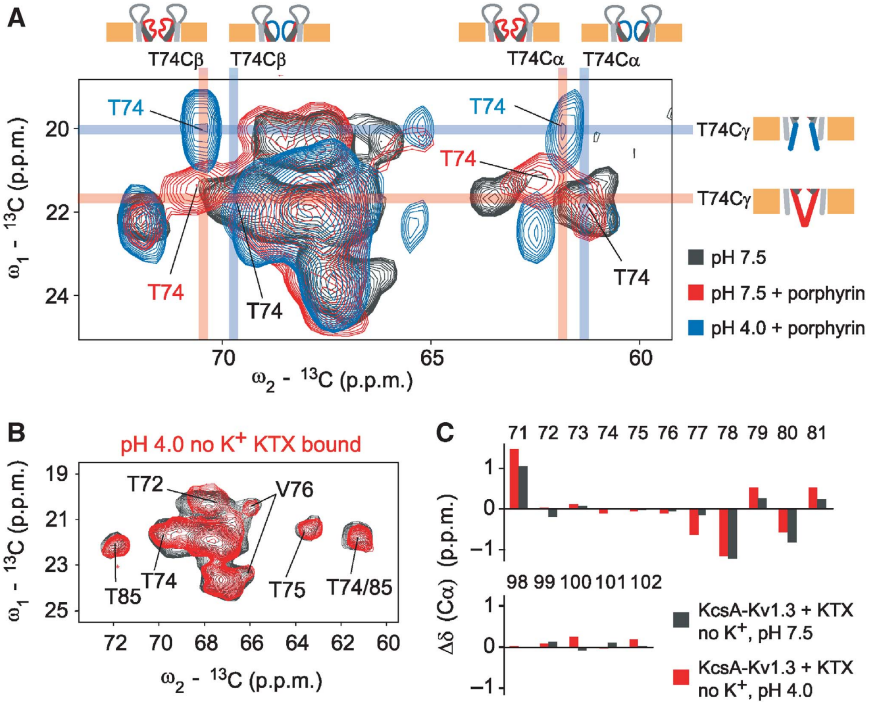


**Figure 4** (**A**) Regions from ($^{13}$C, $^{13}$C) correlation spectra obtained for free KcsA–Kv1.3 at pH 7.5 (black) and bound to porphyrin at pH 7.5 (red) and pH 4.0 (blue). Assignments for T74 Cα, Cβ and Cγ atoms are indicated by coloured bars. Although sizable Cα and Cβ chemical-shift changes are observed for different states of the inactivation gate, namely for conductive and collapsed states of the selectivity filter, the Cγ chemical-shift changes largely on activation-gate opening indicating a coupling of the two gates through side-chain interactions. Drawings indicate gating states as defined in Figure 1D and blue and red mark open and closed states, respectively. (**B**) Regions from ($^{13}$C, $^{13}$C) correlation spectra obtained for KTX-bound KcsA–Kv1.3 at pH 7.5 (black) and pH 4.0 (red). (**C**) Cα chemical-shift changes, in the absence of $K^+$, observed at two pH values for the inactivation gate (residues 71–81) and the activation gate (residues 98–102) of KTX-bound KcsA–Kv1.3 with respect to free KcsA–Kv1.3 at pH 7.5.

**Table I** Summary of channel states observed under different [$K^+$] and pH conditions for free and ligand-bound KcsA-Kv1.3 reconstituted in asolectin liposomes

| [$K^+$] | pH | Free | KTX | Porphyrin |
|---|---|---|---|---|
| *State of the activation gate as seen by ssNMR* | | | | |
| — | 7.5 | Closed | Closed | Closed |
| — | 4.0 | Open | Closed | Open |
| 50 mM | 7.5 | Closed | ND | ND |
| 50 mM | 4.0 | Closed | ND | ND |
| *State of the inactivation gate as seen by ssNMR* | | | | |
| — | 7.5 | Open | Blocked open[a] | Closed |
| — | 4.0 | Closed | Blocked open[a] | Closed |
| 50 mM | 7.5 | Open | ND | ND |
| 50 mM | 4.0 | Open | ND | ND |
| *Protonation state of Glu118/Glu120* | | | | |
| — | 7.5 | Deprotonated | Deprotonated | Deprotonated |
| — | 4.0 | Protonated | Deprotonated | Protonated |
| 50 mM | 7.5 | Deprotonated | ND | ND |
| 50 mM | 4.0 | Deprotonated | ND | ND |
| *Side-chain chemical-shift changes observed for Thr74* | | | | |
| — | 7.5 | No | No | No |
| — | 4.0 | Yes | No | Yes |
| 50 mM | 7.5 | No | ND | ND |
| 50 mM | 4.0 | No | ND | ND |

ND, not determined.
[a]Chemical shift changes indicate adaptation of the selectivity filter conformation due to toxin binding as reported earlier (Lange *et al*, 2006).

open-collapsed conformation at pH 4.0, if the buffer solution contains no or only submillimolar $K^+$ concentrations. Conversely, in high (mM) $K^+$ concentrations, we observed as most stable conformation in asolectin liposomes a closed-conductive state of the KcsA–Kv1.3 channel at pH 7.5 as well as pH 4.0. The $K^+$-sensitive gating transition to the open-inactivated state is correlated with a $K^+$-sensitive protonation of glutamate residues 71, 118 and 120, which have an important influence on selectivity-filter conformation (Glu71) (Cordero-Morales *et al*, 2006b, 2007) and on pH-induced activation-gate opening (Glu118 and 120) (Thompson *et al*, 2008), respectively. Substitution of Glu71 by alanine prevents entry into the inactivated state and essentially abolishes the voltage sensitivity of KcsA gating (Cordero-Morales *et al*, 2006a, 2007). Using ssNMR spectroscopy, we could directly show that protonation of Glu71 correlates with inactivation-gate closure, consistent with a crucial role of this residue in pH, $K^+$ and voltage sensitivity of KcsA inactivation. At the intracellular side of the channel's pore domain, Glu118 and Glu120 (as well as His25) are involved in pH-induced activation-gate opening (Thompson *et al*, 2008). Our ssNMR data show that protonation of Glu118 and 120 correlates with activation-gate opening and that their acid–base equilibrium is $K^+$ sensitive. This underpins the notion that these residues located at the helix bundle crossing are essential elements of the channel's pH sensor.

Our data reveal a higher KcsA–Kv1.3 steady-state current at high external $K^+$ concentrations, a finding that agrees well with earlier studies and is consistent with the idea that C-type inactivation is correlated with the collapse of a conductive selectivity-filter structure (Demo and Yellen, 1991; Baukrowitz and Yellen, 1995; Kiss and Korn, 1998; Ader *et al*, 2008). An earlier study found a $K_D$ of 0.43 mM for $K^+$ binding to the selectivity filter of KcsA (Lockless *et al*, 2007). We found that the $K_D$ value of 0.9 mM for the sensitivity of KcsA–Kv1.3 inactivation to external [$K^+$] as measured by steady-state current is conspicuously similar. In addition, our electrophysiological experiments indicate that an internal high-affinity $K^+$-binding site with a $K_D$ of 6.5 μM modulates KcsA–Kv1.3 activation gating. ssNMR experiments show concordantly that the open KcsA–Kv1.3 activation gate is more stable in low than in high $K^+$ concentrations. These results are favourably complemented by earlier electrophysiological studies on $K^+$-sensitive gating of the KcsA channel (LeMasurier *et al*, 2001; Zakharian and Reusch, 2004). Note that the overall ionic strength, which has been shown to influence channel open probability (Heginbotham *et al*, 1998), was kept constant in our experiments. Such a strategy also eliminates other side effects, for example related to surface potential or mechanical stability of the proteoliposome. Therefore, the observed $K^+$ effects on channel gating can be traced to $K^+$ itself. Earlier reports attributed low channel open-probability at acidic pH to an open-inactivated state as seen in ssNMR experiments in low ($<1$ mM) $K^+$ concentrations (Perozo *et al*, 1999; Liu *et al*, 2001; Blunck *et al*, 2006; Cordero-Morales *et al*, 2006b). In the light of the results presented here, the exact $K^+$ concentrations, most likely also the lipidic environments used (Valiyaveetil *et al*, 2002), seem to be of crucial relevance for comparing results of different structure-based functional studies. It is also important to note that electrochemical gradients as present in electrophysiology have so far not been reproduced in structural studies. For this reason, we have not attempted to study the voltage sensitivity of KcsA–Kv1.3 gating (Cordero-Morales *et al*, 2006a) by ssNMR on a structural level. Conversely, an electrochemical gradient generated either by a gradient of $K^+$ or voltage across the lipid bilayer is obligatory for functional studies by electrophysiology. Thus, our strategy was to combine functional experiments on KcsA–Kv1.3 in asymmetric [$K^+$] and transmembrane voltage conditions with ssNMR data on $K^+$, pH and ligand dependence of KcsA–Kv1.3 steady-state conformation. This allowed us to delineate the influence of $K^+$ on activation and inactivation gates both under equilibrium and non-equilibrium conditions, yielding a coherent picture of KcsA–Kv1.3-channel gating. Although $K^+$-channel gating proceeds through an open-inactivated state, as established in electrophysiological experiments (Figure 1A; Kurata and Fedida, 2006; Chakrapani *et al*, 2007a), our data show that, in the absence of transmembrane voltage, the steady-state conformation of KcsA–Kv1.3 in asolectin liposomes is closed conductive even at pH 4.0 if millimolar ($\geqslant 10$ mM) $K^+$ concentrations are present.

We have earlier shown that ssNMR chemical shift and through-space distance data obtained on KcsA–Kv1.3 at pH 7.5 (Ader *et al*, 2008) are in good agreement with the closed-conductive (C) state of the KcsA channel as seen in the crystal structure (PDB ID 1K4C). There, side chains of residues in pore helix and lower selectivity filter on the one hand, and TM2 gating hinge region on the other hand are in close spatial proximity, possibly forming an interconnected network crucial for gate coupling. We observed in our ssNMR data synchronized pH-dependent chemical-shift changes in side-chain nuclei of residues from both regions, for example Ile100 Cδ1 and Thr75 Cγ2, which are $<5$ Å apart in the KcsA X-ray

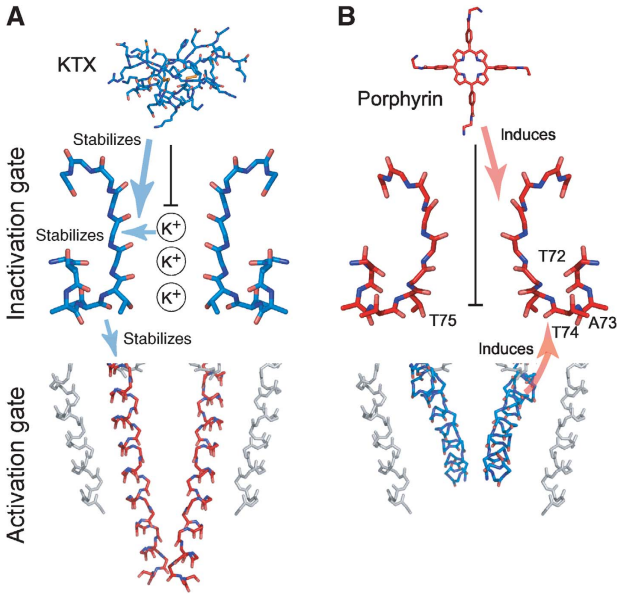


**Figure 5** Overview of $K^+$ and ligand effects influencing the conformation of both channel gates. (**A**) Conductive selectivity filter (blue) and closed activation gate (red) (PDB ID 1K4C) (Zhou *et al*, 2001) as well as KTX (PDB ID 1XSW) (Lange *et al*, 2005). (**B**) Collapsed selectivity filter (red) (PDB ID 1K4D) (Zhou *et al*, 2001) and a model for the open activation gate (blue) as well as porphyrin ligand (Ader *et al*, 2008). KTX and porphyrin stabilize the conductive and collapsed backbone conformation, respectively, and affect a different set of $K^+$-binding sites (black vertical bars). Arrows mark the effects of $K^+$ and ligands on the selectivity-filter conformation and the linked impact on activation gating through gate coupling as discussed in the text.

structure (Zhou *et al*, 2001). This suggests that the respective amino acids are part of such a coupling network and that conformational rearrangements during opening of the activation gate, in which the inner helices swing open, are conveyed to the inactivation gate through the gating hinge region. Although our data at this stage cannot provide a high-resolution structural view of the coupling mechanism, we were able to identify residues that are key players for gate coupling based on chemical-shift changes, suggesting that the two gates interact sterically on the side-chain level.

Titration experiments performed with toxin-bound channels (Figure 5) reveal that the gating states of the inactivation gate can control activation gating. Low [$K^+$] supports an opened activation gate in the absence of KTX, but not in the presence of KTX, which traps the filter in a conductive conformation, favouring a closed activation gate. Hence, we found that KTX binding similar to high [$K^+$] stabilizes a closed activation gate at acidic pH. $K^+$-binding sites 2–4 of the selectivity filter, which are affected by porphyrin, but not by KTX binding (Figure 5), are prime candidates for the internal high-affinity-binding site that influences activation gating as seen by electrophysiological and ssNMR experiments. This notion is further supported by earlier reports showing that presence of $K^+$ in the selectivity filter of Kv channels accelerates activation-gate closure (Hurst *et al*, 1997; Panyi and Deutsch, 2006). Thus, it is likely that gate coupling as proposed conveys ligand and $K^+$ sensitivity from the inactivation gate to the activation gate. An intriguing implication of our data is that $K^+$ sensitivity and gate coupling provide a powerful mechanism to adjust the gating cycle based on the relative stability of all four possible gating states, suggesting a scenario for consecutive gating transitions involving opening, closing and inactivation.

## Materials and methods

### *Sample preparation*

KcsA–Kv1.3 expression, purification and reconstitution into asolectin liposomes was carried out as described earlier (Lange *et al*, 2006). Reconstitution was performed at a 100/1 asolectin/KcsA–Kv1.3 molar ratio in either 50 mM Na phosphate, pH 7.5, 50 mM NaCl or 10 mM MOPS, pH 7.0, 150 mM KCl. C-terminally truncated KcsA–Kv1.3 (residues 1–125) was obtained by chymotrypsin digestion. KTX and porphyrin were added in two-fold molar excess as described earlier (Lange *et al*, 2006; Ader *et al*, 2008). pH and $K^+$ titrations were performed by washing the proteoliposomal pellet three times with 1 ml citrate or phosphate buffer of desired pH and [$K^+$] followed by 30 min ultracentrifugation at 45 000 r.p.m. and $+4^\circ$C. For each titration step, the loss of sample was below 5% as judged from 1D $^{13}$C spectra. Thus, titrations with up to 10 steps could be performed using a single proteoliposomal sample.

### *ssNMR*

All NMR experiments were conducted using 4 mm triple-resonance ($^1$H,$^{13}$C,$^{15}$N) probeheads at static magnetic fields of 9.4, 14.1 and 18.8 T corresponding to 400, 600 and 800 MHz proton-resonance frequencies (Bruker Biospin, Karlsruhe/Germany). Assignments were obtained earlier (Schneider *et al*, 2008) and were extended and verified using 2D ($^{13}$C, $^{13}$C) correlation experiments using proton-driven spin diffusion under weak coupling conditions (Seidel *et al*, 2004). Water-edited ssNMR experiments were performed at 9.4 T and analysed as described elsewhere (Ader *et al*, 2009b) using a 3 ms Gaussian $\pi/2$ pulse, a $T_2$ filter containing two delays ($\tau$) of 1 ms and a crosspolarization contact time of 700 μs. MAS speeds used were 6.5, 9.375 and 12.5 kHz at 9.4, 14.1 and 18.8 T static magnetic field strengths, respectively, at an effective sample temperature of approximately $+7^\circ$C. Integration of spectral cross-peaks was performed using the software Topspin 2.1 (Bruker Biospin, Karlsruhe/Germany). Error estimates for spectral integrals were obtained from integrals in noise regions with sizes equal to those of the signal integration regions.

### *Electrophysiology*

Electrophysiological measurements on KcsA–Kv1.3 in proteoliposomes were performed as described earlier (Ader *et al*, 2008), except that we varied internal and external $K^+$ concentrations in patch-clamp recordings as follows. External (pipette) and internal (bath) solutions contained 10 mM MOPS buffer and 150 mM monovalent cation ($Na^+$ or $K^+$). As indicated in the legends, $K^+$ concentration in external (pipette) or internal (bath) solution was varied from 0 to 150 mM keeping total monovalent cation concentration constant.

### *Supplementary data*

Supplementary data are available at *The EMBO Journal* Online (http://www.embojournal.org).

## Acknowledgements

Technical assistance by B Angerstein is gratefully acknowledged. We are indebted to R Wagner for invaluable support in context of the lipid-bilayer reconstitution experiments. In addition, we thank D Trauner for making the porphyrin pore blocker available to us. This work was funded in part by the DFG (Be 2345/5-1, Ba 1700/8-1, Po 137/28-2) and NWO, by a PhD fellowship to CA from the Stiftung Stipendien-Fonds des Verbands der Chemischen Industrie and by a PhD fellowship to RS from the DFG graduate school 782 'Spectroscopy and Dynamics of Molecular Coils and Aggregates'.

## Conflict of interest

The authors declare that they have no conflict of interest.

## References


Ader C, Pongs O, Becker S, Baldus M (2009a) Protein dynamics detected in a membrane-embedded potassium channel using two-dimensional solid-state NMR spectroscopy. *Biochim Biophys Acta, Biomembr* (doi:10.1016/j.bbamem.2009.06.023)

Ader C, Schneider R, Hornig S, Velisetty P, Wilson EM, Lange A, Giller K, Ohmert I, Martin-Eauclaire M-F, Trauner D, Becker S, Pongs O, Baldus M (2008) A structural link between inactivation and block of a $K^+$ channel. *Nat Struct Mol Biol* **15:** 605–612

Ader C, Schneider R, Seidel K, Etzkorn M, Becker S, Baldus M (2009b) Structural rearrangements of membrane proteins probed by water-edited solid-state NMR spectroscopy. *J Am Chem Soc* **131:** 170–176

Armstrong CM (2003) Voltage-gated K channels. *Sci STKE* **2003:** re10

Baker KA, Tzitzilonis C, Kwiatkowski W, Choe S, Riek R (2007) Conformational dynamics of the KcsA potassium channel governs gating properties. *Nat Struct Mol Biol* **14:** 1089–1095

Baukrowitz T, Yellen G (1995) Modulation of $K^+$ current by frequency and external $[K^+]$: a tale of two inactivation mechanisms. *Neuron* **15:** 951–960

Baukrowitz T, Yellen G (1996) Use-dependent blockers and exit rate of the last ion from the multi-ion pore of a $K^+$ channel. *Science* **271:** 653–656

Ben-Abu Y, Zhou Y, Zilberberg N, Yifrach O (2009) Inverse coupling in leak and voltage-activated $K^+$ channel gates underlies distinct roles in electrical signaling. *Nat Struct Mol Biol* **16:** 71–79

Bernèche S, Roux B (2005) A gate in the selectivity filter of potassium channels. *Structure* **13:** 591–600

Blunck R, Cordero-Morales JF, Cuello LG, Perozo E, Bezanilla F (2006) Detection of the opening of the bundle crossing in KcsA with fluorescence lifetime spectroscopy reveals the existence of two gates for ion conduction. *J Gen Physiol* **128:** 569–581

Chakrapani S, Cordero-Morales JF, Perozo E (2007a) A quantitative description of KcsA gating I: macroscopic currents. *J Gen Physiol* **130:** 465–478

Chakrapani S, Cordero-Morales JF, Perozo E (2007b) A quantitative description of KcsA gating II: single-channel currents. *J Gen Physiol* **130:** 479–496

Claydon TW, Vaid M, Rezazadeh S, Kwan DCH, Kehl SJ, Fedida D (2007) A direct demonstration of closed-state inactivation of $K^+$ channels at low pH. *J Gen Physiol* **129:** 437–455

Cordero-Morales JF, Cuello LG, Perozo E (2006a) Voltage-dependent gating at the KcsA selectivity filter. *Nat Struct Mol Biol* **13:** 319–322

Cordero-Morales JF, Cuello LG, Zhao Y, Jogini V, Cortes DM, Roux B, Perozo E (2006b) Molecular determinants of gating at the potassium-channel selectivity filter. *Nat Struct Mol Biol* **13:** 311–318

Cordero-Morales JF, Jogini V, Lewis A, Vasquez V, Cortes DM, Roux B, Perozo E (2007) Molecular driving forces determining potassium channel slow inactivation. *Nat Struct Mol Biol* **14:** 1062–1069

Cuello LG, Romero JG, Cortes DM, Perozo E (1998) pH-dependent gating in the streptomyces lividans $K^+$ channel. *Biochemistry* **37:** 3229–3236

Demo SD, Yellen G (1991) The inactivation gate of the Shaker $K^+$ channel behaves like an open-channel blocker. *Neuron* **7:** 743–753

Doyle DA, Morais Cabral J, Pfuetzner RA, Kuo A, Gulbis JM, Cohen SL, Chait BT, MacKinnon R (1998) The structure of the potassium channel: molecular basis of $K^+$ conduction and selectivity. *Science* **280:** 69–77

Gao L, Mi X, Paajanen V, Wang K, Fan Z (2005) From the cover: activation-coupled inactivation in the bacterial potassium channel KcsA. *Proc Natl Acad Sci USA* **102:** 17630–17635

Heginbotham L, Kolmakova-Partensky L, Miller C (1998) Functional reconstitution of a prokaryotic $K^+$ channel. *J Gen Physiol* **111:** 741–749

Heginbotham L, LeMasurier M, Kolmakova-Partensky L, Miller C (1999) Single Streptomyces lividans $K^+$ channels: functional asymmetries and sidedness of proton activation. *J Gen Physiol* **114:** 551–560

Hille B (ed) (2001) *Ion Channels of Excitable Membranes*, 3rd edn, Sinauer: Sunderland, Mass

Holmgren M, Shin KS, Yellen G (1998) The activation gate of a voltage-gated $K^+$ channel can be trapped in the open state by an intersubunit metal bridge. *Neuron* **21:** 617–621

Hurst RS, Roux MJ, Toro L, Stefani E (1997) External barium influences the gating charge movement of Shaker potassium channels. *Biophys J* **72:** 77–84

Jiang Y, Lee A, Chen J, Cadene M, Chait BT, MacKinnon R (2002a) Crystal structure and mechanism of a calcium-gated potassium channel. *Nature* **417:** 515–522

Jiang Y, Lee A, Chen J, Cadene M, Chait BT, MacKinnon R (2002b) The open pore conformation of potassium channels. *Nature* **417:** 523–526

Keim P, Vigna RA, Morrow JS, Marshall RC, Gurd FRN (1973) Carbon 13 nuclear magnetic resonance of pentapeptides of glycine containing central residues of serine, threonine, aspartic and glutamic acids, asparagine, and glutamine. *J Biol Chem* **248:** 7811–7818

Kelly BL, Gross A (2003) Potassium channel gating observed with site-directed mass tagging. *Nat Struct Mol Biol* **10:** 280–284

Kiss L, Korn SJ (1998) Modulation of C-type inactivation by $K^+$ at the potassium channel selectivity filter. *Biophys J* **74:** 1840–1849

Kurata HT, Fedida D (2006) A structural interpretation of voltage-gated potassium channel inactivation. *Prog Biophys Mol Biol* **92:** 185–208

Lange A, Becker S, Seidel K, Giller K, Pongs O, Baldus M (2005) A concept for rapid protein-structure determination by solid-state NMR spectroscopy. *Angew Chem Int Ed* **44:** 2089–2092

Lange A, Giller K, Hornig S, Martin-Eauclaire M-F, Pongs O, Becker S, Baldus M (2006) Toxin-induced conformational changes in a potassium channel revealed by solid-state NMR. *Nature* **440:** 959–962

Legros C, Pollmann V, Knaus H-G, Farrell AM, Darbon H, Bougis PE, Martin-Eauclaire M-F, Pongs O (2000) Generating a high affinity scorpion toxin receptor in KcsA-Kv1.3 chimeric potassium channels. *J Biol Chem* **275:** 16918–16924

Legros C, Schulze C, Garcia ML, Bougis PE, Martin-Eauclaire MF, Pongs O (2002) Engineering-specific pharmacological binding sites for peptidyl inhibitors of potassium channels into KcsA. *Biochemistry* **41:** 15369–15375

LeMasurier M, Heginbotham L, Miller C (2001) KcsA: it's a potassium channel. *J Gen Physiol* **118:** 303–314

Lenaeus MJ, Vamvouka M, Focia PJ, Gross A (2005) Structural basis of TEA blockade in a model potassium channel. *Nat Struct Mol Biol* **12:** 454–459

Liu Y, Holmgren M, Jurman ME, Yellen G (1997) Gated access to the pore of a voltage-dependent $K^+$ channel. *Neuron* **19:** 175–184

Liu Y, Jurman ME, Yellen G (1996) Dynamic rearrangement of the outer mouth of a $K^+$ channel during gating. *Neuron* **16:** 859–867

Liu Y-S, Sompornpisut P, Perozo E (2001) Structure of the KcsA channel intracellular gate in the open state. *Nat Struct Mol Biol* **8:** 883–887

Lockless SW, Zhou M, MacKinnon R (2007) Structural and thermodynamic properties of selective ion binding in a $K^+$ channel. *PLoS Biol* **5:** e121

Ogielska EM, Aldrich RW (1999) Functional consequences of a decreased potassium affinity in a potassium channel pore. Ion interactions and C-type inactivation. *J Gen Physiol* **113:** 347–358

Panyi G, Deutsch C (2006) Cross talk between activation and slow inactivation gates of shaker potassium channels. *J Gen Physiol* **128:** 547–559

Panyi G, Deutsch C (2007) Probing the cavity of the slow inactivated conformation of shaker potassium channels. *J Gen Physiol* **129:** 403–418

Perozo E, Cortes DM, Cuello LG (1998) Three-dimensional architecture and gating mechanism of a $K^+$ channel studied by EPR spectroscopy. *Nat Struct Mol Biol* **5:** 459–469

Perozo E, Cortes MD, Cuello LG (1999) Structural rearrangements underlying $K^+$-channel activation gating. *Science* **285:** 73–78

Roeper J, Lorra C, Pongs O (1997) Frequency-dependent inactivation of mammalian A-type $K^+$ channel KV1.4 regulated by $Ca^{2+}$/calmodulin-dependent protein kinase. *J Neurosci* **17:** 3379–3391

Schneider R, Ader C, Lange A, Giller K, Hornig S, Pongs O, Becker S, Baldus M (2008) Solid-state NMR spectroscopy applied to a chimeric potassium channel in lipid bilayers. *J Am Chem Soc* **130:** 7427–7435

Schrempf H, Schmidt O, Kummerlen R, Hinnah S, Muller D, Betzler M, Steinkamp T, Wagner R (1995) A prokaryotic potassium ion channel with two predicted transmembrane segments from Streptomyces lividans. *EMBO J* **14:** 5170–5178

Seidel K, Lange A, Becker S, Hughes CE, Heise H, Baldus M (2004) Protein solid-state NMR resonance assignments from ($^{13}C$,$^{13}C$) correlation spectroscopy. *Phys Chem Chem Phys* **6:** 5090–5093

Takeuchi K, Takahashi H, Kawano S, Shimada I (2007) Identification and characterization of the slowly exchanging pH-dependent conformational rearrangement in KcsA. *J Biol Chem* **282:** 15179–15186

Thompson AN, Posson DJ, Parsa PV, Nimigean CM (2008) Molecular mechanism of pH sensing in KcsA potassium channels. *Proc Natl Acad Sci USA* **105:** 6900–6905

Valiyaveetil FI, Zhou Y, MacKinnon R (2002) Lipids in the structure, folding, and function of the KcsA $K^+$ channel. *Biochemistry* **41:** 10771–10777

Yellen G (1998) The moving parts of voltage-gated ion channels. *Q Rev Biophys* **31:** 239–295

Zachariae U, Schneider R, Velisetty P, Lange A, Seeliger D, Wacker SJ, Karimi-Nejad Y, Vriend G, Becker S, Pongs O, Baldus M, de Groot BL (2008) The molecular mechanism of toxin-induced conformational changes in a potassium channel: relation to C-type inactivation. *Structure* **16:** 747–754

Zagotta WN, Aldrich RW (1990) Voltage-dependent gating of Shaker A-type potassium channels in Drosophila muscle. *J Gen Physiol* **95:** 29–60

Zakharian E, Reusch RN (2004) Streptomyces lividans potassium channel KcsA is regulated by the potassium electrochemical gradient. *Biochem Biophys Res Commun* **316:** 429–436

Zheng J, Sigworth FJ (1997) Selectivity changes during activation of mutant shaker potassium channels. *J Gen Physiol* **110:** 101–117

Zhou Y, Morais-Cabral JH, Kaufman A, MacKinnon R (2001) Chemistry of ion coordination and hydration revealed by a $K^+$ channel-Fab complex at 2.0 resolution. *Nature* **414:** 43–48

 